Influence of Grain Structure and Doping on the Deformation and Fracture of Polycrystalline Silicon for MEMS/NEMS

Ioannis Chasiotis
Aerospace Engineering
University of Illinois at Urbana-Champaign

AFOSR Grant # FA9550-09-1-0535
Program Manager: Dr. B.L. Lee

Report Documentation Page

Form Approved
OMB No. 0704-0188

1. REPORT DATE **AUG 2012**	2. REPORT TYPE	3. DATES COVERED **00-00-2012 to 00-00-2012**

4. TITLE AND SUBTITLE **Influence of Grain Structure and Doping on the Deformation and Fracture of Polycrystalline Silicon for MEMS/NEMS**	5a. CONTRACT NUMBER 5b. GRANT NUMBER 5c. PROGRAM ELEMENT NUMBER
6. AUTHOR(S)	5d. PROJECT NUMBER 5e. TASK NUMBER 5f. WORK UNIT NUMBER
7. PERFORMING ORGANIZATION NAME(S) AND ADDRESS(ES) **University of Illinois at Urbana-Champaign,Aerospace Engineering,Urbana,IL,61801**	8. PERFORMING ORGANIZATION REPORT NUMBER
9. SPONSORING/MONITORING AGENCY NAME(S) AND ADDRESS(ES)	10. SPONSOR/MONITOR'S ACRONYM(S) 11. SPONSOR/MONITOR'S REPORT NUMBER(S)

12. DISTRIBUTION/AVAILABILITY STATEMENT
Approved for public release; distribution unlimited

13. SUPPLEMENTARY NOTES
Presented at the 2nd Multifunctional Materials for Defense Workshop in conjunction with the 2012 Annual Grantees'/Contractors' Meeting for AFOSR Program on Mechanics of Multifunctional Materials & Microsystems Held 30 July - 3 August 2012 in Arlington, VA. Sponsored by AFRL, AFOSR, ARO, NRL, ONR, and ARL. U.S. Government or Federal Rights License

14. ABSTRACT

15. SUBJECT TERMS

16. SECURITY CLASSIFICATION OF:			17. LIMITATION OF ABSTRACT	18. NUMBER OF PAGES	19a. NAME OF RESPONSIBLE PERSON
a. REPORT **unclassified**	b. ABSTRACT **unclassified**	c. THIS PAGE **unclassified**	**Same as Report (SAR)**	**29**	

Standard Form 298 (Rev. 8-98)
Prescribed by ANSI Std Z39-18

Goals, Accomplishments, On-going Research

Research Objectives

- Investigate the dependence of mode I fracture toughness of polysilicon thin films on grain size and doping
- Quantify mechanical strength size effects for laminated and columnar grain polysilicon subjected to different doping conditions.

Accomplishments

- Measured the effective mode I critical stress intensity factor for laminated and columnar grain polysilicon films as a function of dopant concentration
- Quantified the effect of specimen size on fracture strength of polysilicon films via a Weibull analysis to identify the location of failure initiation
- Employed fusion bonded (Si-Si) chevron notch specimens to study the effect of doping and crystallographic orientation on K_{IC} of Si grain boundaries
- Characterized the electromechanical behavior of PZT thin films for MEMS.

On-going Research

- Measure the K_{IC} of polysilicon grain boundaries as a function of dopant concentration with fracture experiments on Si-Si wafer bonded specimens with Chevron notches
- Removal of sidewall defects in columnar grain polysilicon to determine the improvement in mechanical strength.

Fabrication of Columnar and Laminated Polysilicon

Columnar Polysilicon

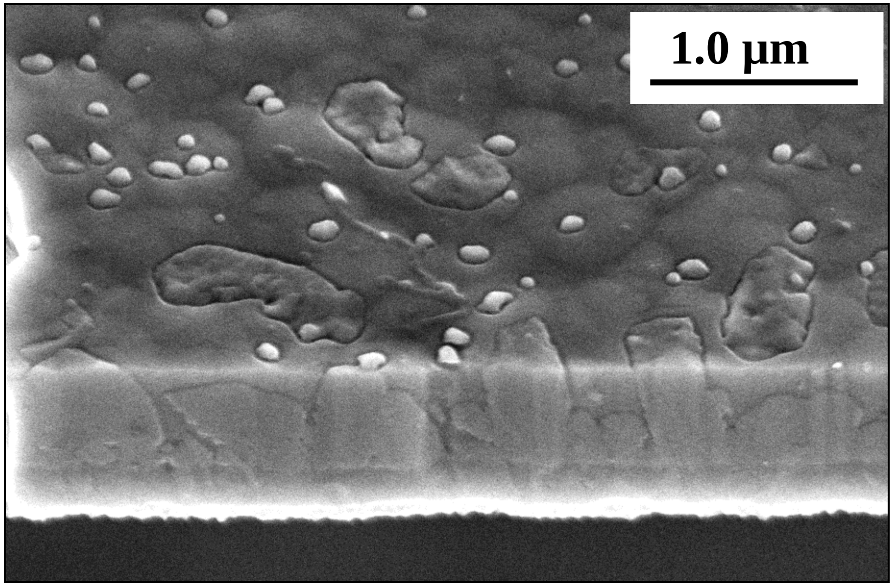

Laminated Polysilicon

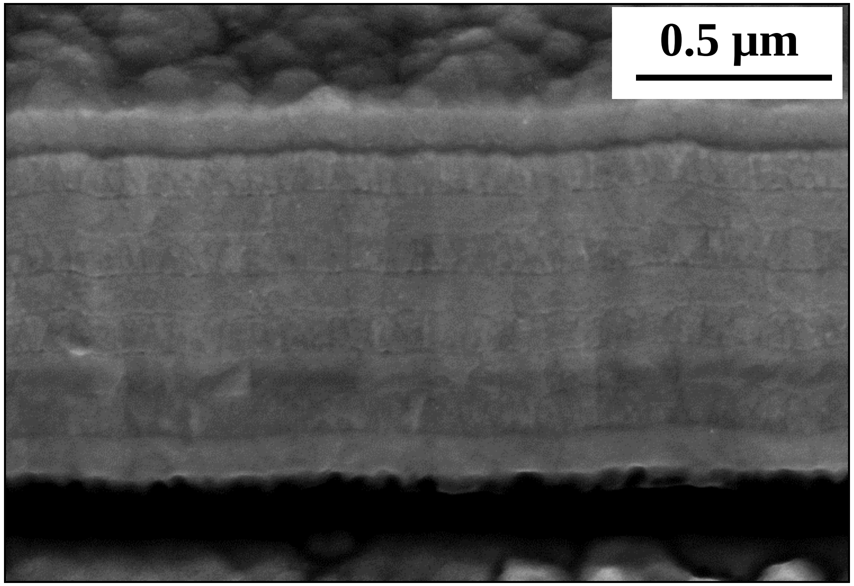

- Polysilicon films were fabricated using a modified Sandia's SUMMiT V^{TM} microfabrication process.
- 1 μm thick polysilicon films were micromachined into dog-bone shaped specimens with gage length and width of 1,000 μm and 100 μm respectively.
- Both polysilicon types of film were doped with various concentrations of P diffused from a sacrificial phosphosilicate glass (PSG) layer during annealing.

Fabrication of Columnar and Laminated Polysilicon

Columnar Polysilicon

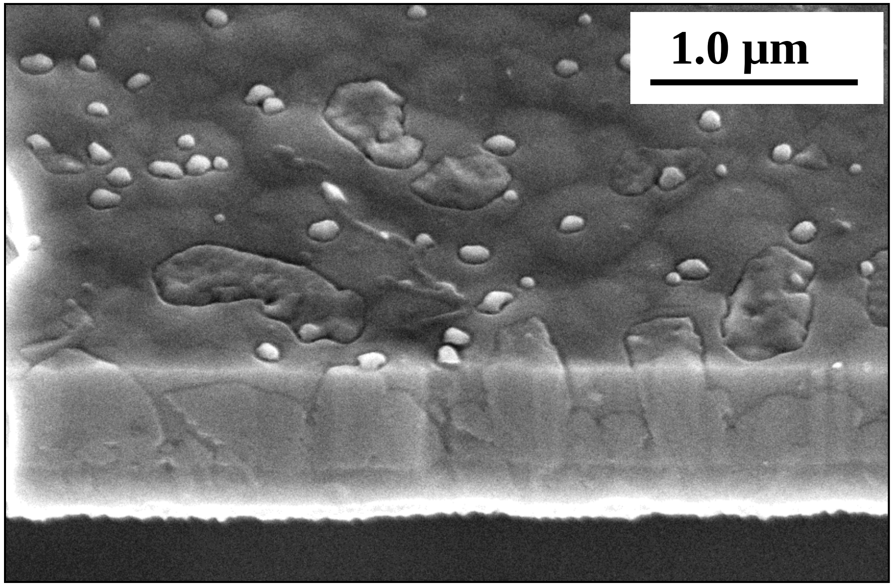

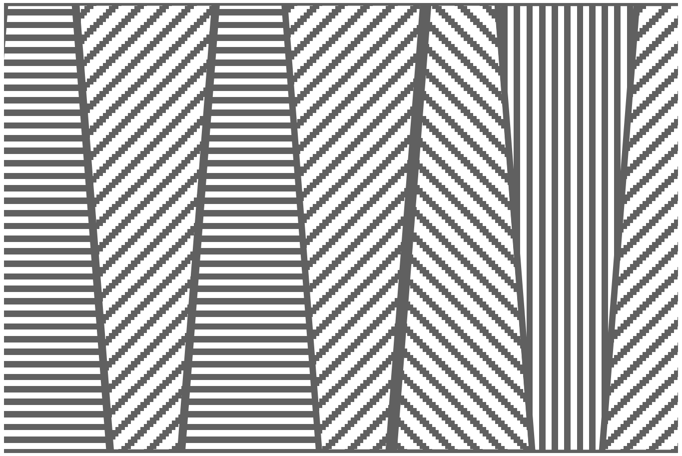

Laminated Polysilicon

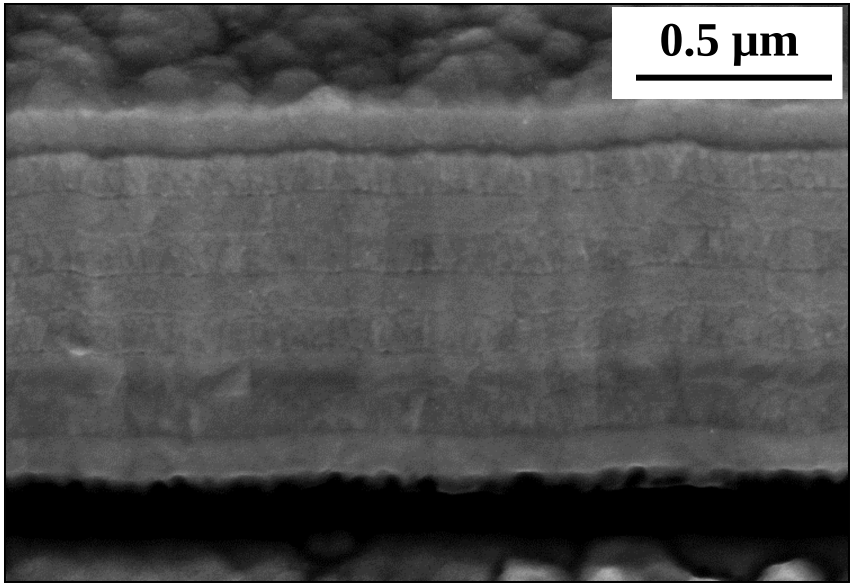

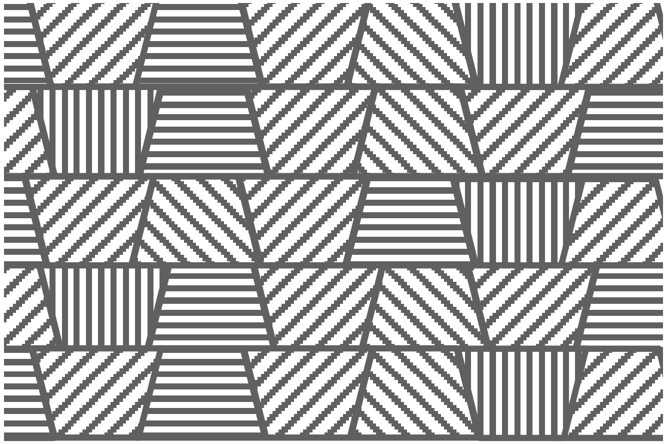

Polysilicon Films with Different Grain Size and Doping

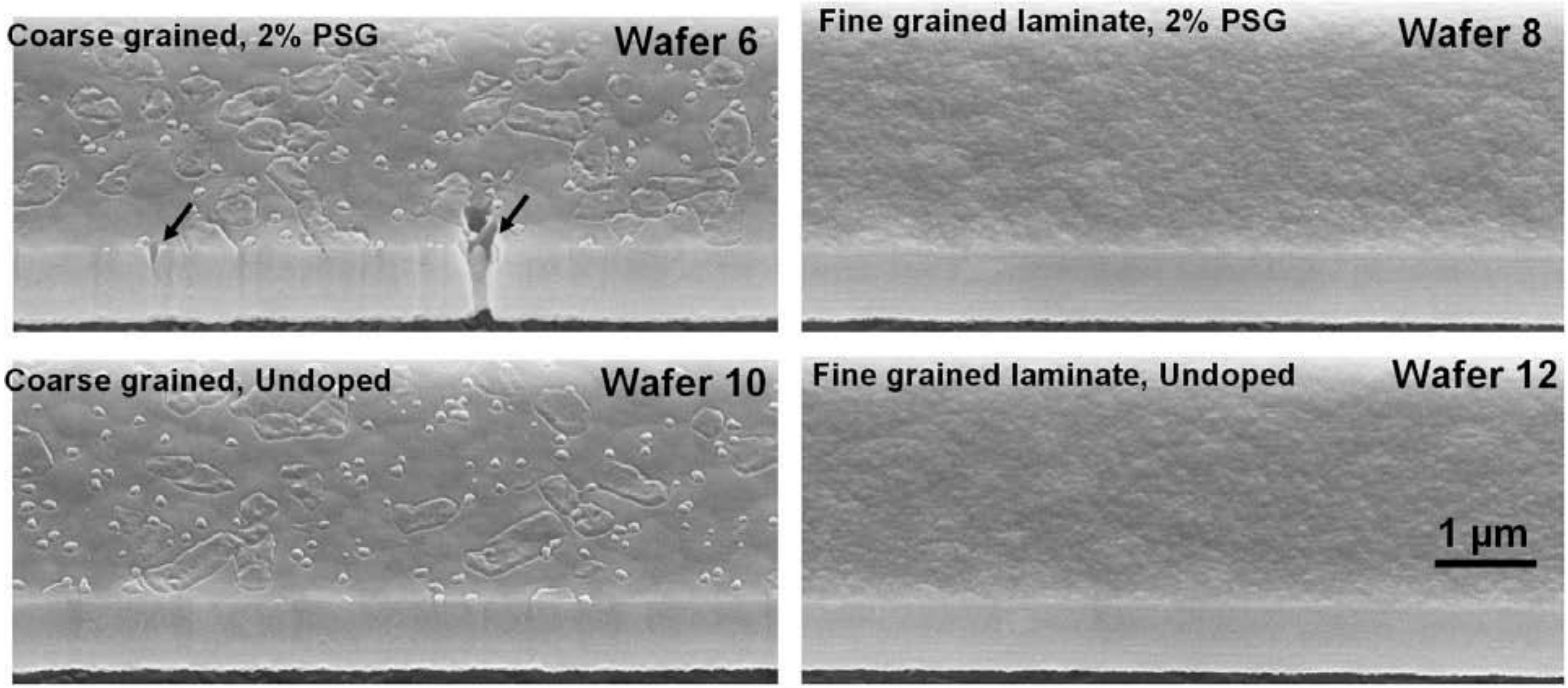

- Polysilicon film specimens (1 µm thick) were fabricated in a special run at the Sandia National Laboratories
- Two types of polysilicon films : Large grain and small grain (laminated)
- The laminar structure controlled the grain size.

B.L. Boyce, et al., “Stronger silicon for microsystems”, Acta Materialia 58, pp. 439-448, (2010)

Fracture Specimens for Microscale Experiments

- Mathematically sharp cracks were generated by indentation performed on the substrate near a specimen free edge
- Edge cracks with an average length of 25 µm were introduced to 1 µm thin polysilicon specimens
- Cracks were imaged by SEM and AFM to obtain their geometry and the grain structure at the crack tip.

Indentation to create edge crack in polycrystalline silicon thin film specimens

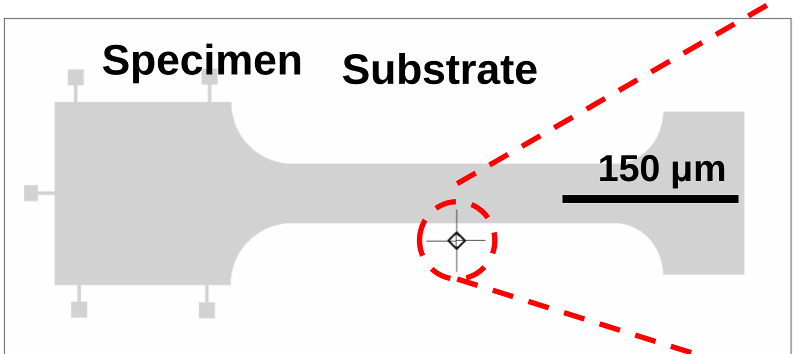

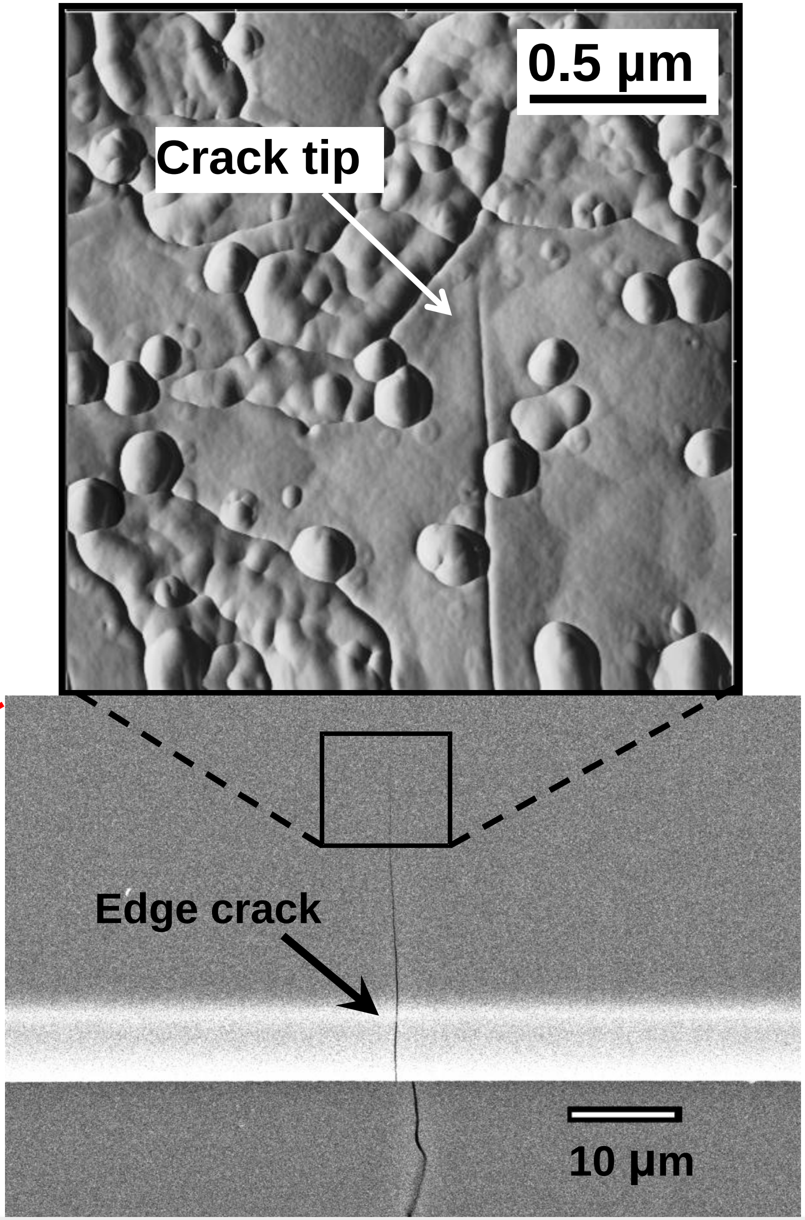

I. Chasiotis, S.W. Cho, K. Jonnalagadda, "Fracture Toughness and Crack Growth in Polycrystalline Silicon", Journal of Applied Mechanics 73 (5) , pp. 714-722, (2006).

Crack Tip in Polysilicon Films with Different Grain Structures

Columnar polySi, 2% PSG

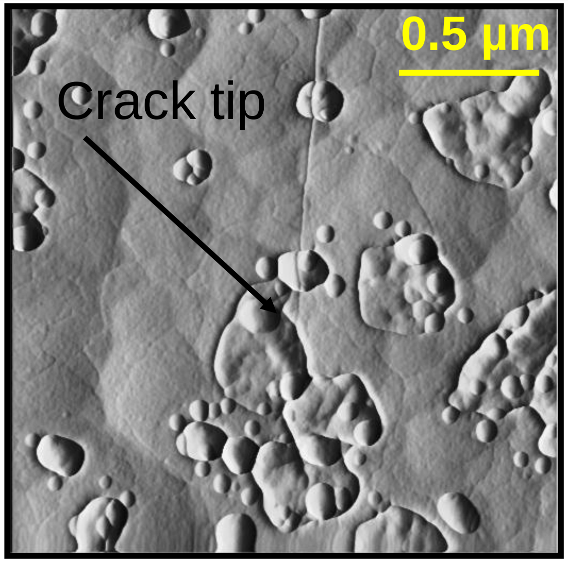

Laminated polySi, 2% PSG

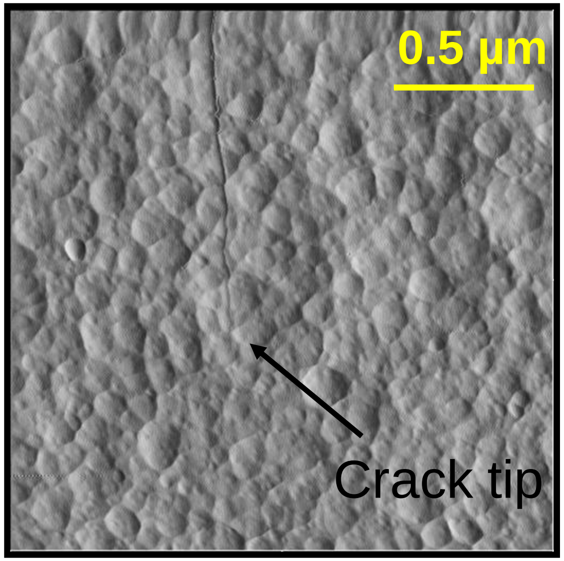

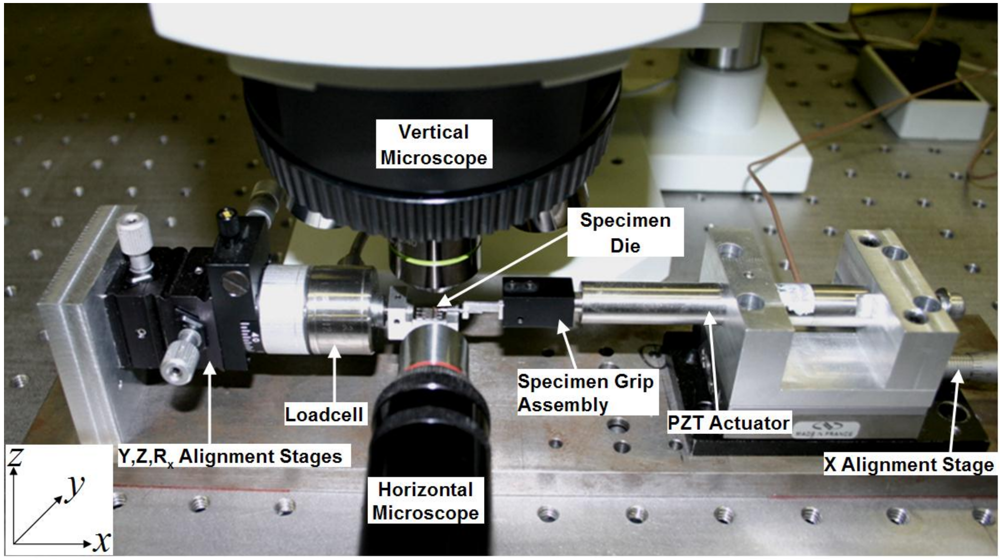

- The precise location of the crack tip, its geometry and adjacent material were determined using AFM images obtained at different magnifications
- Experimental setup used to test pre-cracked polysilicon thin films under mode I loading.

K. Jonnalagadda, I. Chasiotis, S. Yagnamurthy J. Lambros, R. Polcawich, J. Pulskamp, and M. Dubey, "Experimental Investigation of Strain Rate Dependence in Nanocrystalline Pt Films," Experimental Mechanics 50 (1), pp. 25-35, (2010).

Effect of Grain Structure and Doping on $K_{IC,eff}$

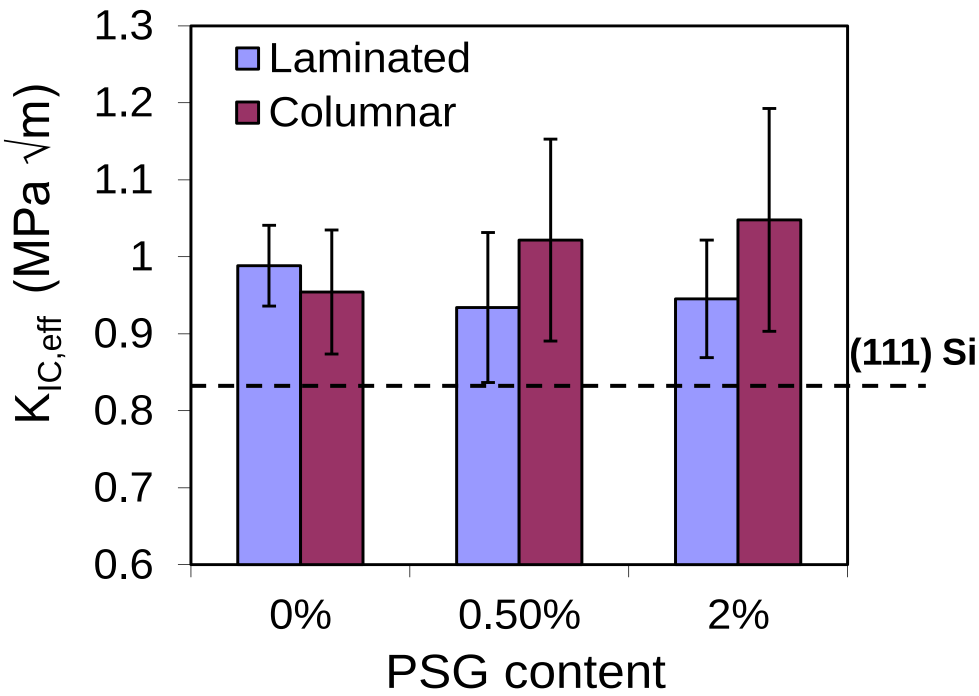

$K_{IC,eff}$ (MPa√m)	Laminated	Columnar
Undoped	0.99±0.05	0.95±0.08
0.5% PSG	0.93±0.10	1.02±0.13
2% PSG	0.97±0.08	1.05±0.14

- $K_{IC,eff}$ of columnar polysilicon was higher than that of laminated polysilicon.
- Minimum K_{IC} for single crystal silicon is 0.84 MPa√m
- Phosphorous atoms diffuse into substitutional sites in Si forming P-Si bonds that have higher bond energy: bond energies of Si-Si and P-Si are 326.86 kJmol^{-1} and 363.6 kJmol^{-1} respectively.

Sub-Critical Crack Growth in Columnar Polysilicon

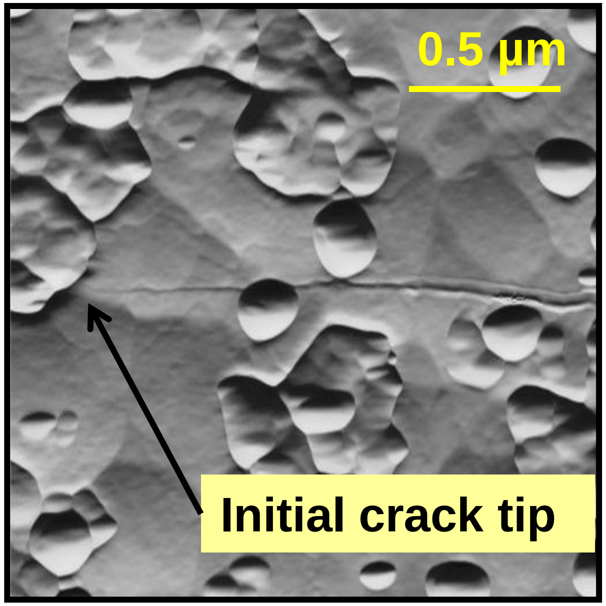

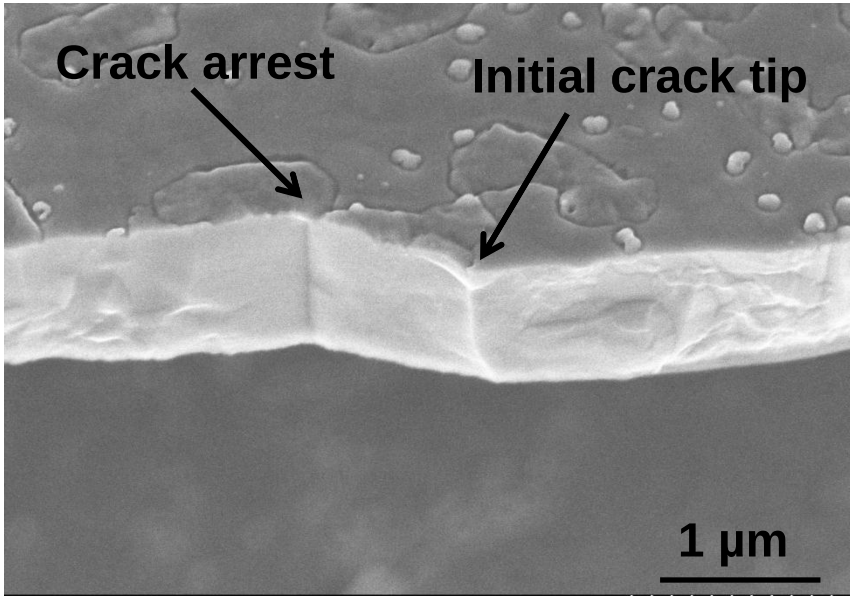

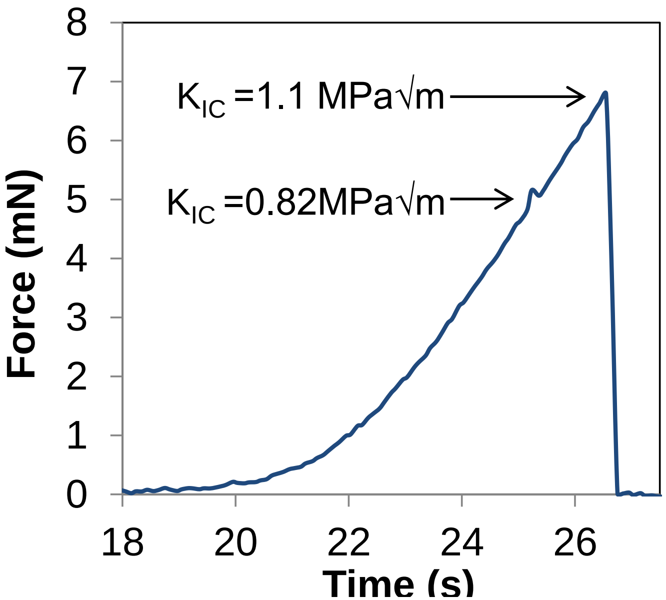

- Local crack tip deflection was observed in heavily doped (2%) large grain polysilicon
- Initial crack propagation was along the most energetically favorable plane, with the crack subsequently arrested at a grain boundary.

Grain Structure and Doping Effect on Fracture Strength

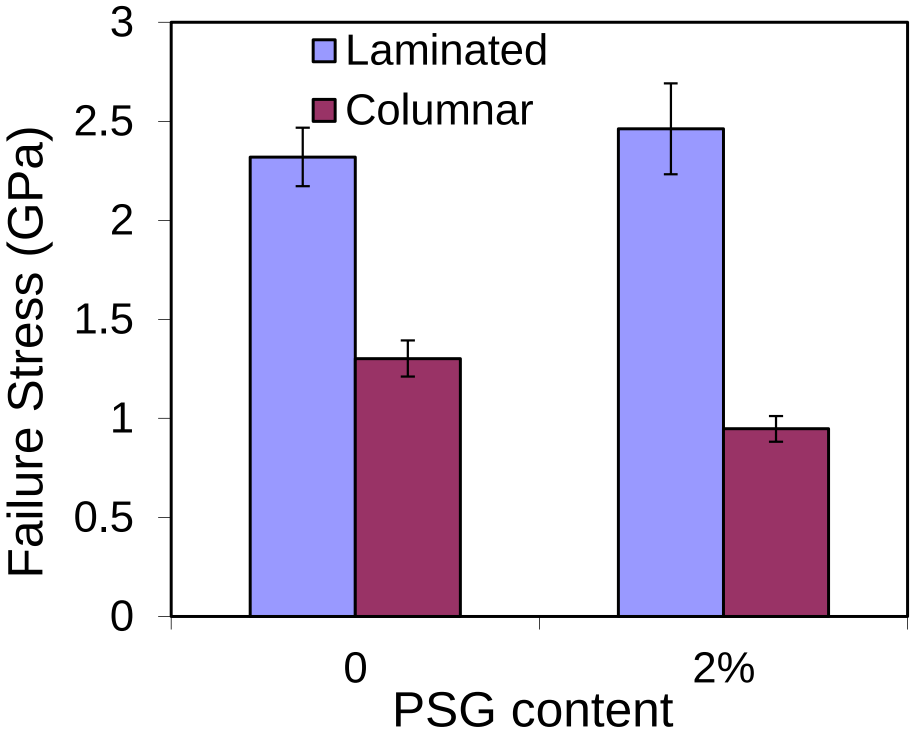

Average strength of polysilicon

	Undoped (GPa)	2% PSG (GPa)
Laminated (~125nm)	2.32±0.15	2.46±0.22
Columnar (~285nm)	1.30±0.09	0.95±0.07

- The fracture strength of laminated polysilicon was 80-150% higher than columnar
- Heavily doped columnar polysilicon film exhibited ~25% lower fracture strength compared to undoped
- This implies that the increase in the upper bound of K_{IC} is due to crack kinking.

Critical Defects on Sidewalls of Columnar Polysilicon

Columnar polysilicon (undoped)

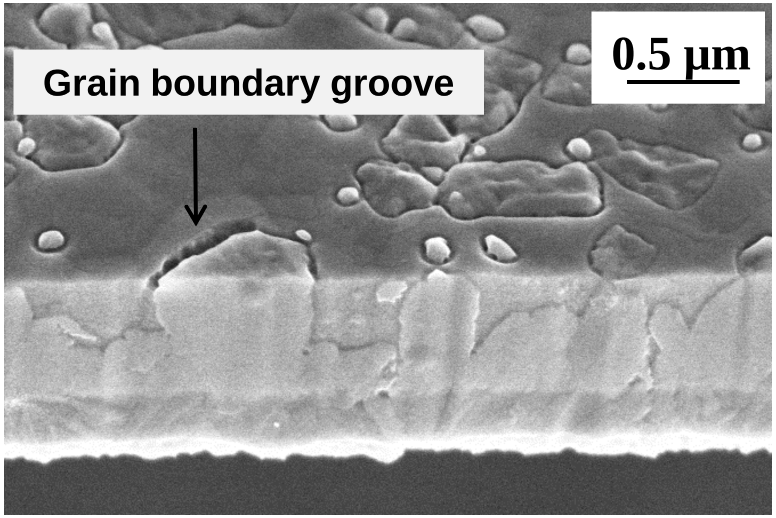

Laminated polysilicon

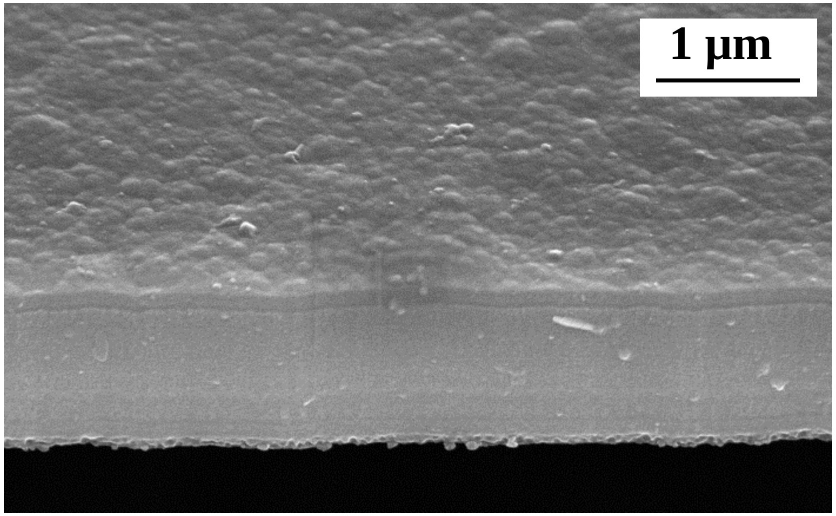

Columnar polysilicon (2% PSG)

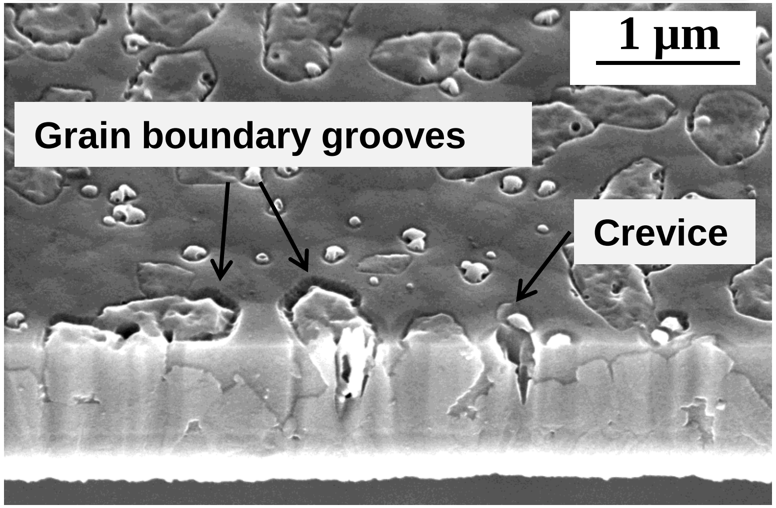

- 100-300 nm deep crevices were found on the side walls of heavily doped columnar polysilicon films.
- Doping had no impact on the surface of laminated polysilicon films.

Scaling of Mechanical Strength of Polysilicon

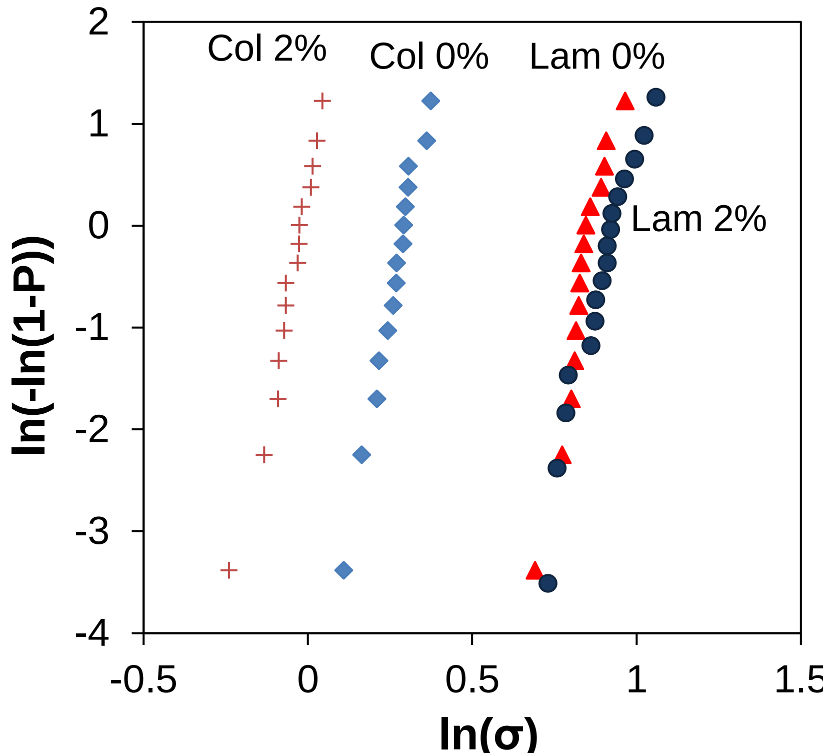

$$P = 1 - \exp\left(-\left(\frac{\sigma - \sigma_0}{\sigma_c} \right)^m \right)$$

σ – measured strength
σ_c – characteristic strength
σ_o – smallest failure stress
m – Weibull modulus

Our study   Boyce et al (specimens ~180 times smaller)

	0% Columnar	2% Columnar	0% Laminated	2% Laminated
σ_c (GPa)	1.34	1.01	2.32	2.51
m	17.63	16.89	10.314	9.09
σ_c (GPa)	1.76	1.48	2.80	2.83
m	12.9	8.7	8.6	13.5

Scaling of Mechanical Strength of Polysilicon

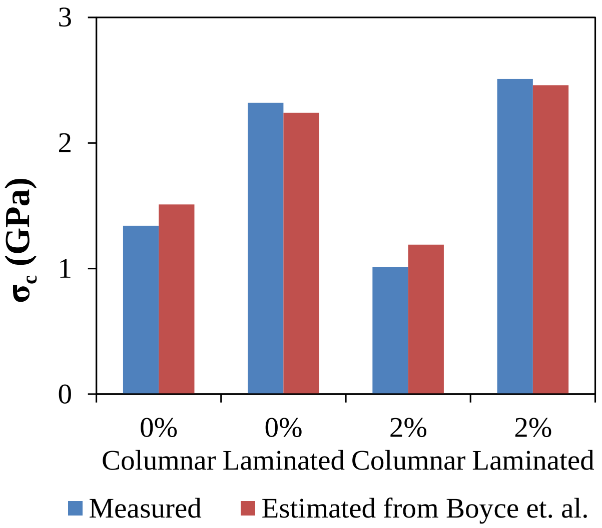

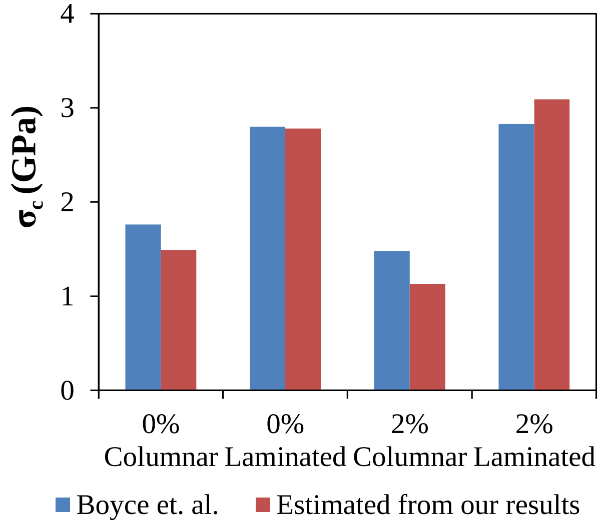

$$\sigma_{c2} = \sigma_{c1} \times \left(\frac{A_1}{A_2} \right)^{\frac{1}{m}}$$

A_n is side wall area

Defects scale with side wall area

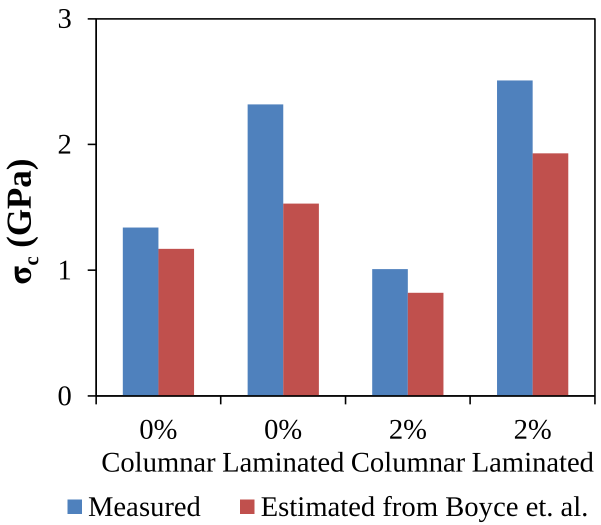

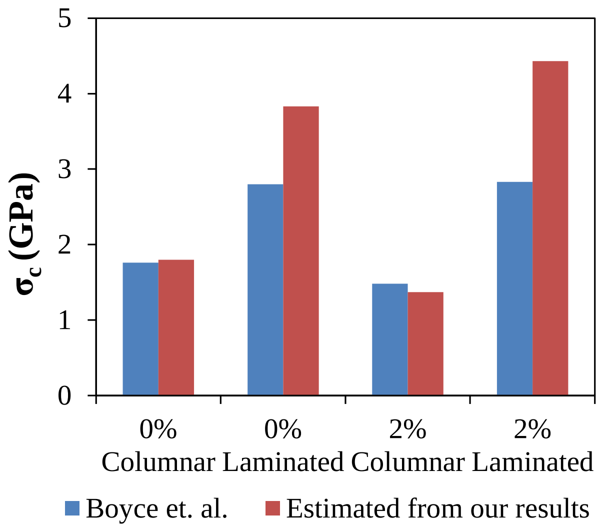

$$\sigma_{c2} = \sigma_{c1} \times \left(\frac{A_1}{A_2} \right)^{\frac{1}{m}}$$

A_n is top surface area

Comparison with Existing Polysilicon Processes

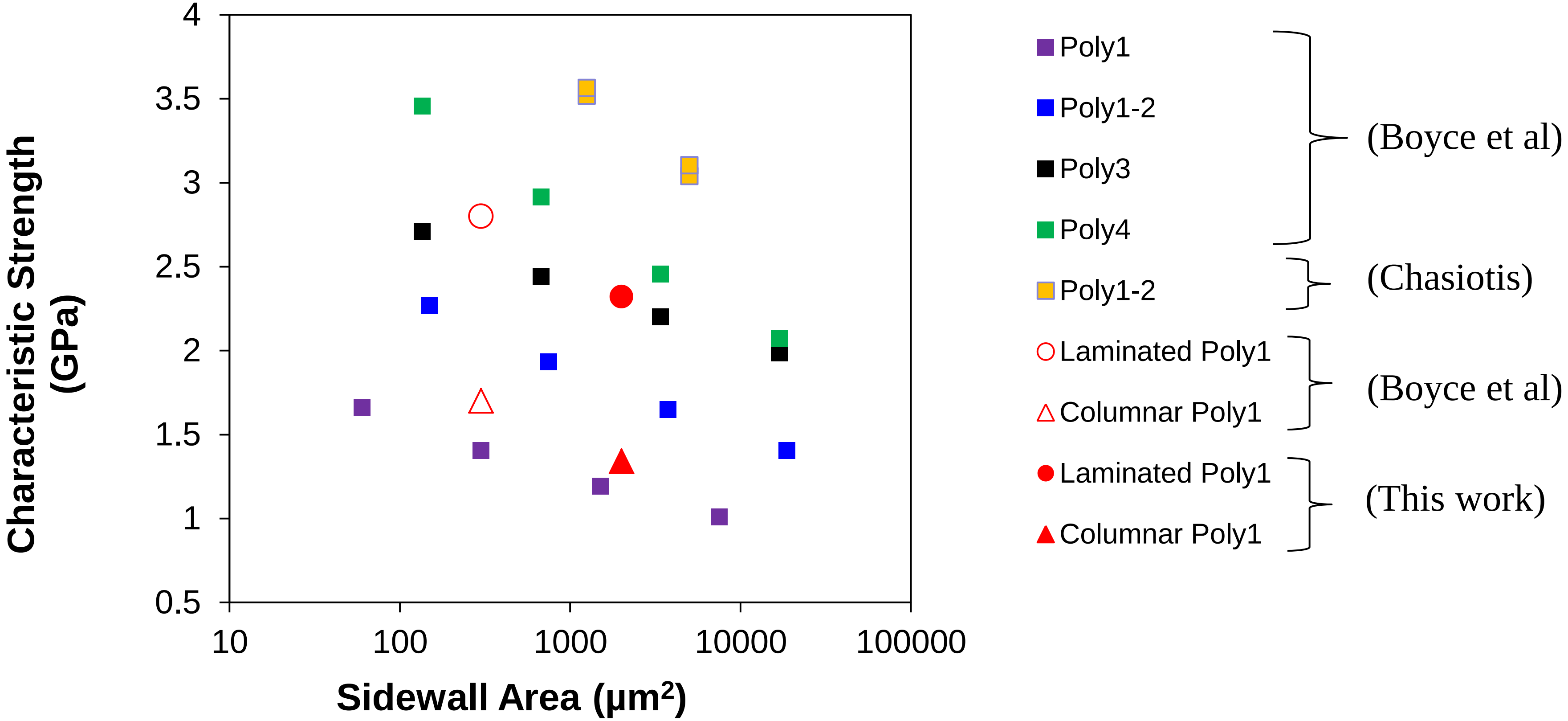

The characteristic strength of laminated poly1 improved and matched that of poly3, whereas the strength of columnar poly1 is comparable to that of regular poly1.

- I. Chasiotis, W.G. Knauss, Journal of the Mechanics and Physics of Solids 51, pp. 1551-1572, (2003).
- B. Boyce, et al, “Strength Distributions in Polycrystalline Silicon MEMS”, JMEMS, 16, pp. 179-190, 2007
- B.L. Boyce, et al., “Stronger silicon for microsystems”, Acta Materialia 58, pp. 439–448 (2010)

Columnar Polysilicon with Defect Free Sidewalls

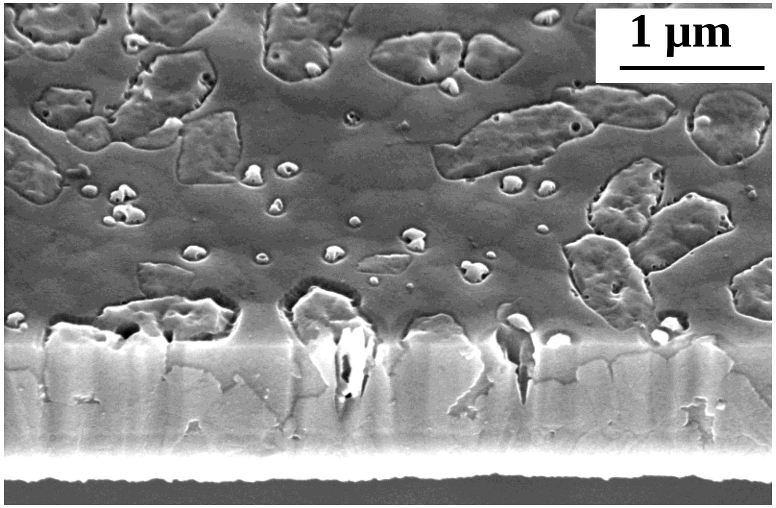

Side walls machined using FIB

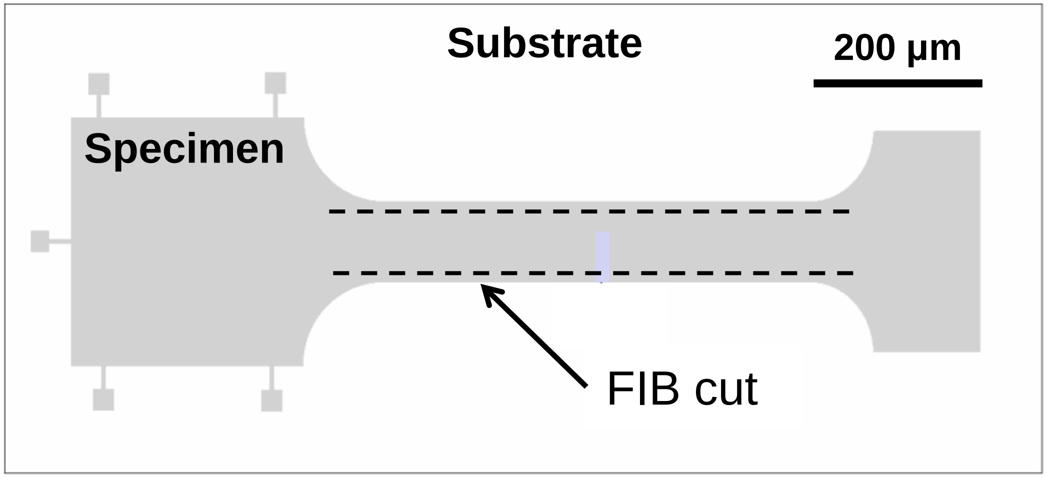

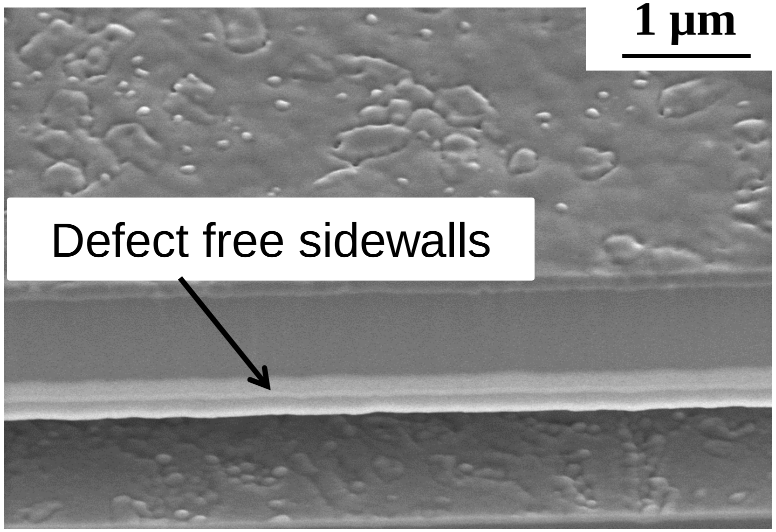

Columnar polysilicon, 2% PSG

- Sidewalls of columnar polysilicon were machined using FIB to fabricate defect free specimens
- Currently resolving challenges in gripping the specimens to test them in uniaxial tension using the narrow section.

Ongoing Work: Cohesive Law for Silicon Grain Boundaries

Chevron notch specimens

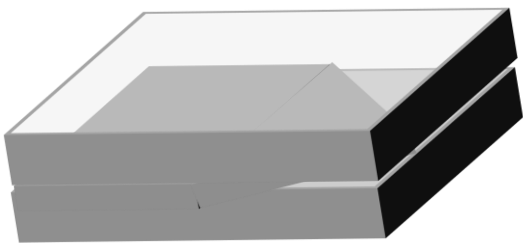

Top view

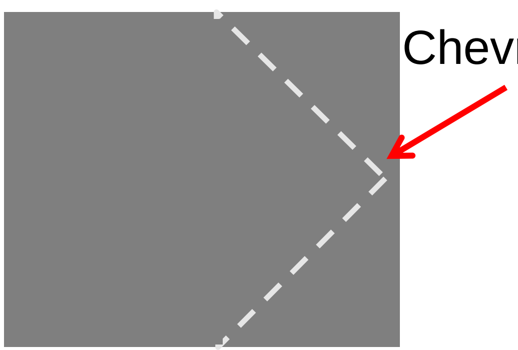

Chevron tip

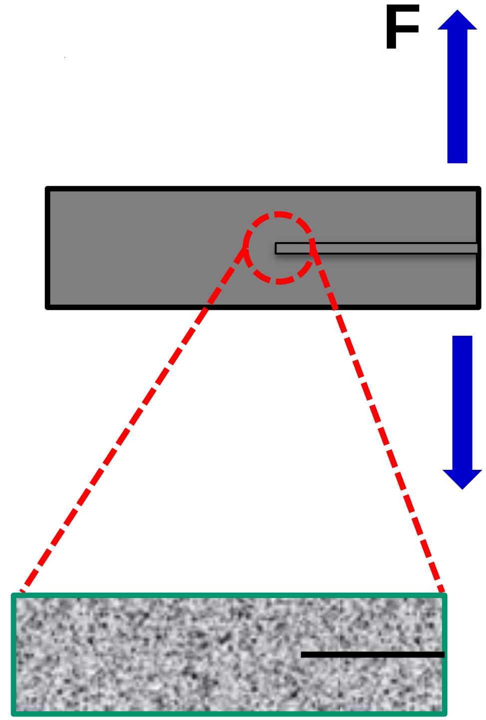

DIC of chevron tip for CTOD

Traction separation law

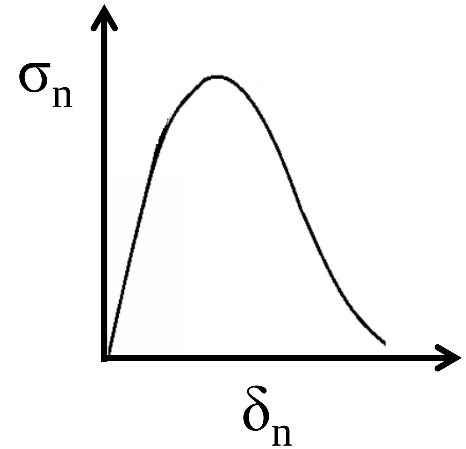

$$\sigma(\delta_n) = \frac{\partial J}{\partial \delta_n}$$

Traction separation law for the polysilicon grain boundaries obtained from J integral and CTOD measured using DIC.

Effect of Doping on K_{IC} of Si Toughness

Indentation using Vickers tip

Top View

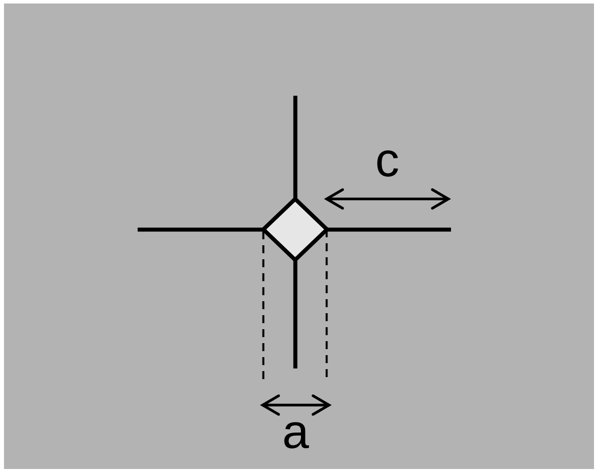

For median cracks with *c/a* >2,

$$K_{\mathrm{Ic}} = 0.129\ (c/a)^{-3/2}\ (\phi E_{[hkl]}/H)^{2/5}\ (Ha^{1/2}/\phi)$$

where $E_{[hkl]}$ is the Young's modulus along [hkl], H is the hardness of Si, φ is a plastic constraint factor (~3).

$$1/E_{[hkl]} = S_{11} - 2(S_{11} - s_{12} - 1/2S_{44})\gamma_{\alpha\beta\theta}$$

$$\gamma_{\alpha\beta\theta} = \mathrm{Cos}^2\ \alpha\ \mathrm{Cos}^2\ \beta + \mathrm{Cos}^2\ \beta\ \mathrm{Cos}^2\ \theta + \mathrm{Cos}^2\ \theta\ \mathrm{Cos}^2\ \alpha$$

$$\mathrm{Cos}\ \alpha = h/(h^2+k^2+l^2)^{\frac{1}{2}},\ \mathrm{Cos}\ \beta = k/(h^2+k^2+l^2)^{\frac{1}{2}},\ \mathrm{Cos}\ \theta = l/(h^2+k^2+l^2)^{\frac{1}{2}}$$

F. Ebrahimi, and L. Kalwani, Mat. Sci. Eng. : A, 268 (1-2), 1999

Indentation will be performed on silicon wafers doped with different concentrations of P

Effect of doping on K_{IC} of different Si planes is being studied by driving median cracks along [001], [110] and [111] directions.

K_{IC} Measurement of Si-Si Interface Strength

Chevron notch specimens

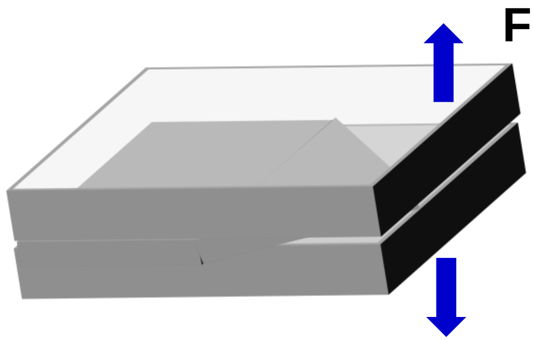

Top view

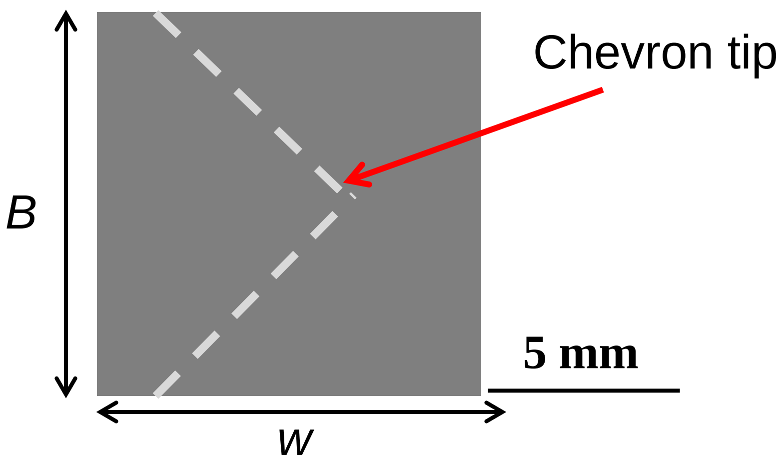

K_I for a chevron notch

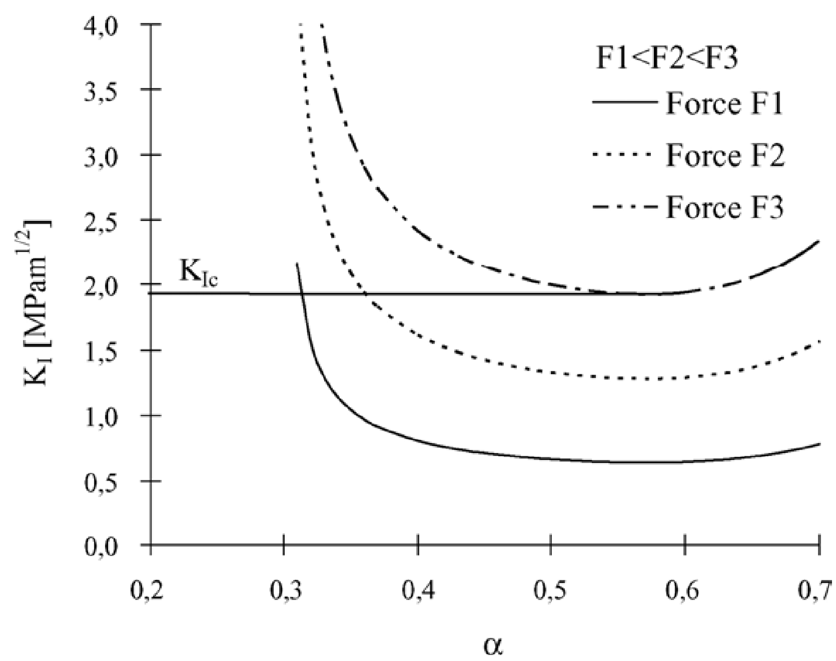

$$K_C = \frac{F_{max}}{B\sqrt{w}} Y_{min}$$

O. Vallin et al, Mater. Sci. Eng., 50, 2005

Fracture toughness of Si – Si interfaces is measured using chevron notch specimens

Fabrication of Chevron Notch Specimens

silicon wafer

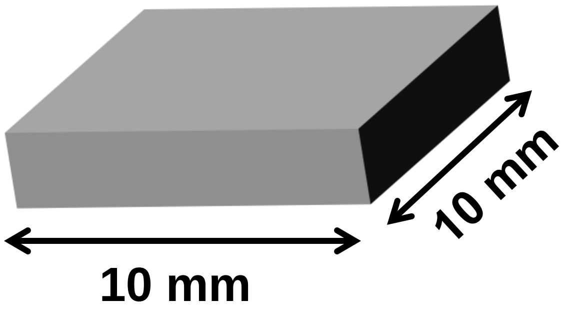

Spin coat photoresist

Photolithography

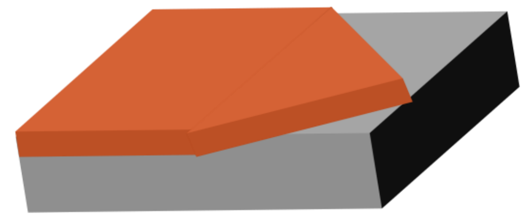

Pattern Si wafer using Bosch's process

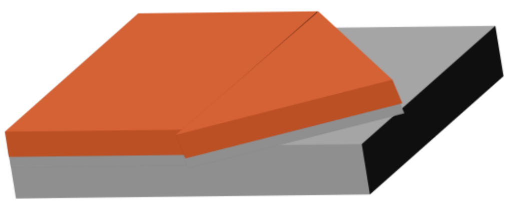

Patterned silicon wafer

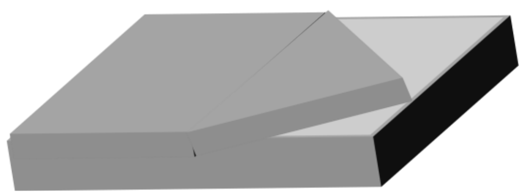

Direct bonding of Si wafers

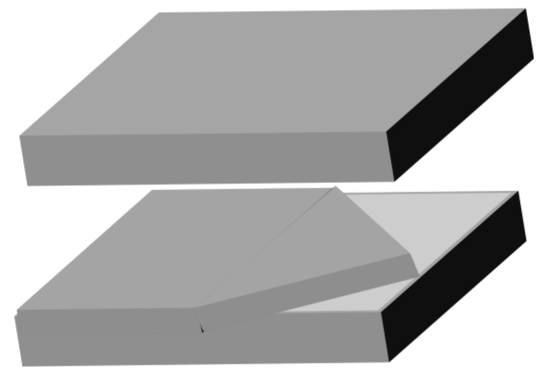

Fusion bonded silicon wafers with different concentrations of P are used to study the effect of P doping on fracture toughness of Si-Si interfaces

Characterization of Si-Si Bond Interface

IR image of crack tip

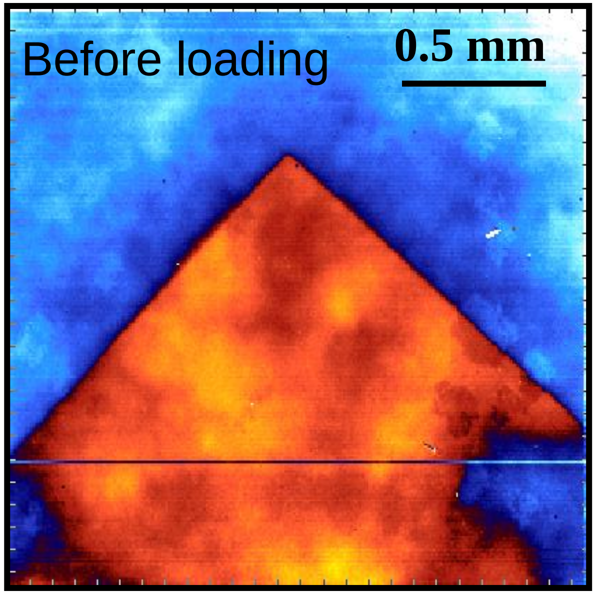

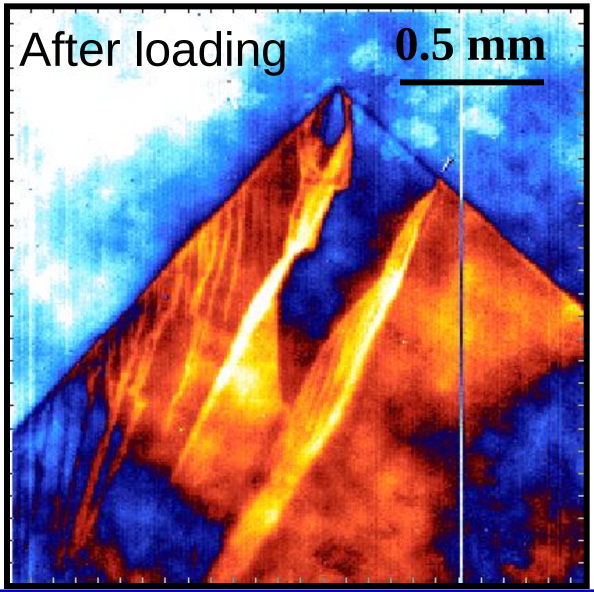

Optical image of fracture plane

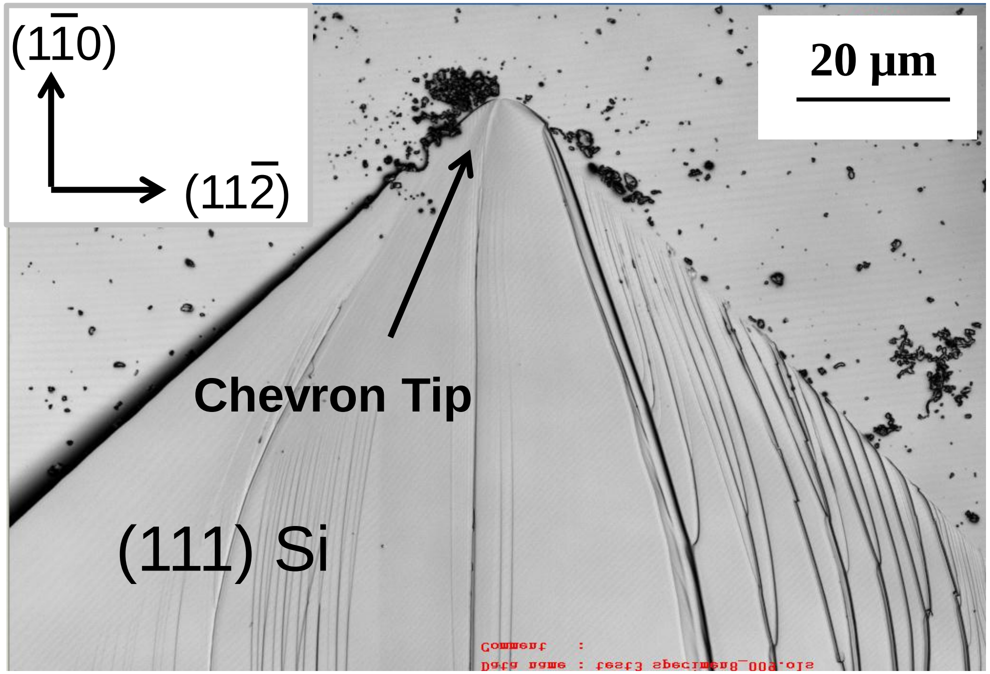

- IR images are used to characterize the quality of the interface
- Silicon cleaves easily on (111) planes and along [110] direction.

Characterization of Si-Si Bond Interface

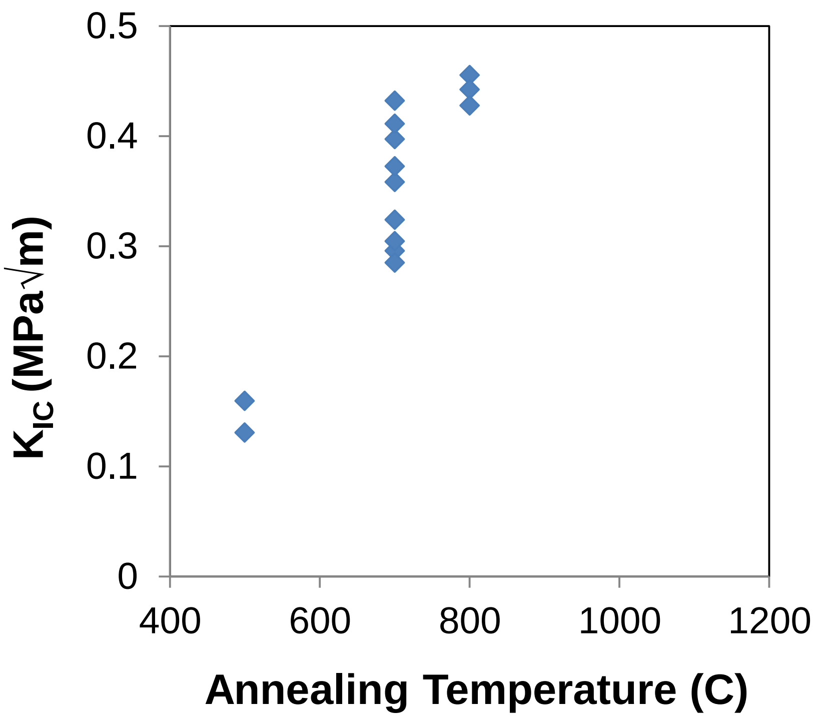

Fracture through the interface

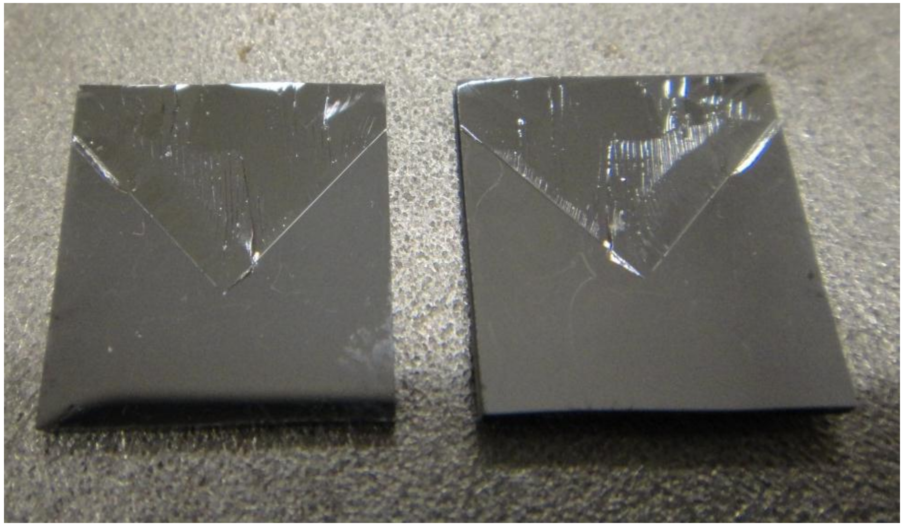

- Strength of Si-Si bond interface is dependent on annealing temperature
- Si-Si interface with different concentrations of P, and crystal orientations are being fabricated and tested to understand their effect on K_{IC} of silicon.

Mechanical & Ferroelectric Behavior of PZT Films for MEMS

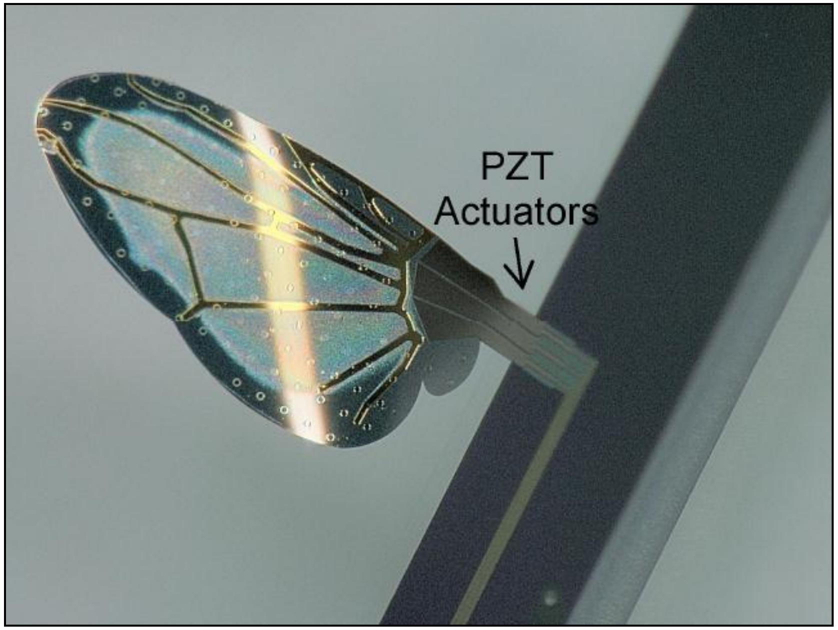

PZT thin film bimorph for MAV* wing

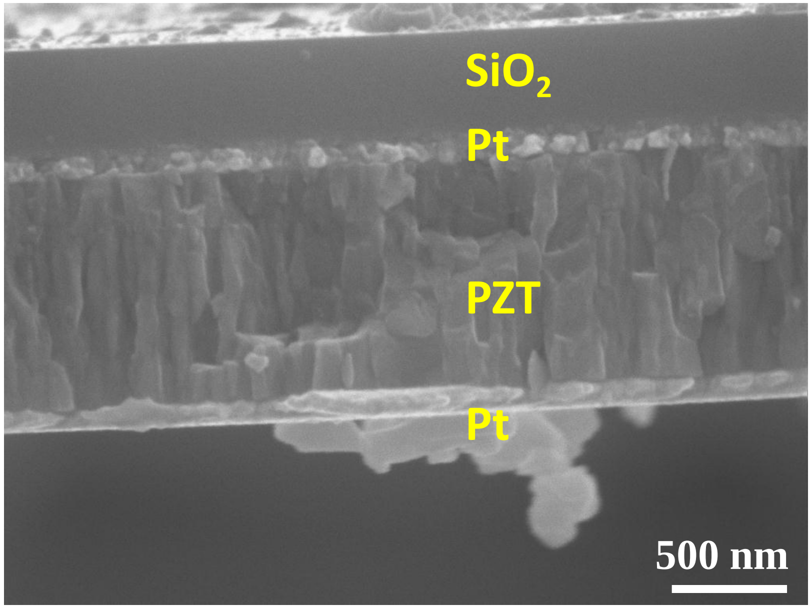

Cross section of SiO_2-Pt-PZT-Pt

- PZT thin films are used in MEMS devices, such as micro-sensors, actuators, and RF-MEMS
- Always fabricated in combination with other films as stacks, they undergo non-standard thermal processing
- Their mechanical and failure properties in PZT stacks are either unknown or widely scattered
- Knowledge of ferroelectric behavior is key in designing reliable devices.

J. Pulskamp et al., Proc. ASME, IDETC/CIE (2009), San Diego, DETC2009-87231

Microscale Measurements

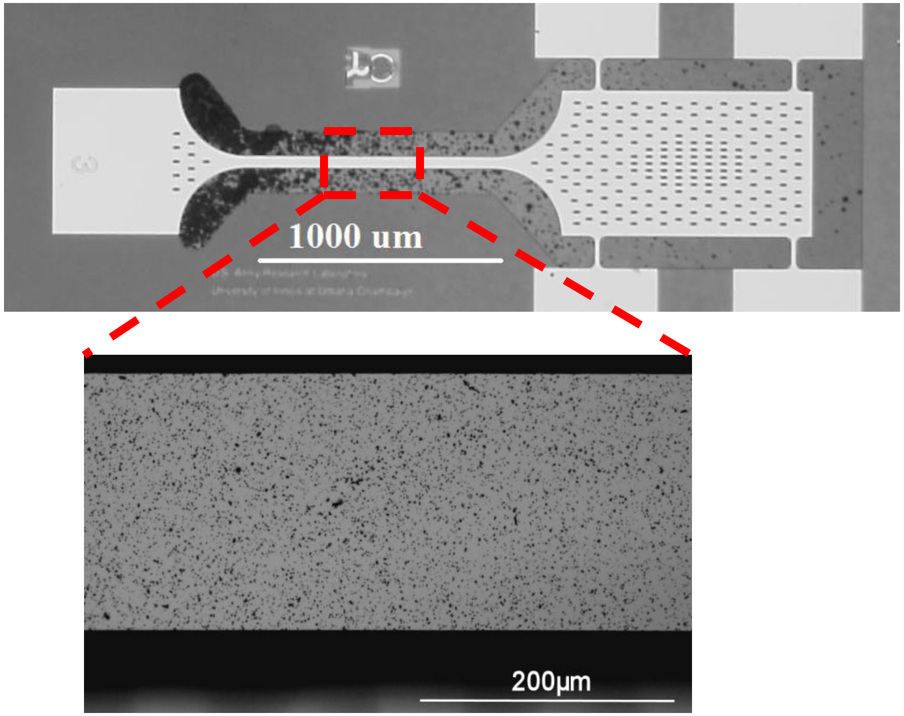

Speckle pattern for direct strain measurement

- Specimens were loaded in uniaxial tension
- Strain was calculated by DIC from the speckle pattern on the samples
- Displacement resolution ~25 nm.

Axial displacement field

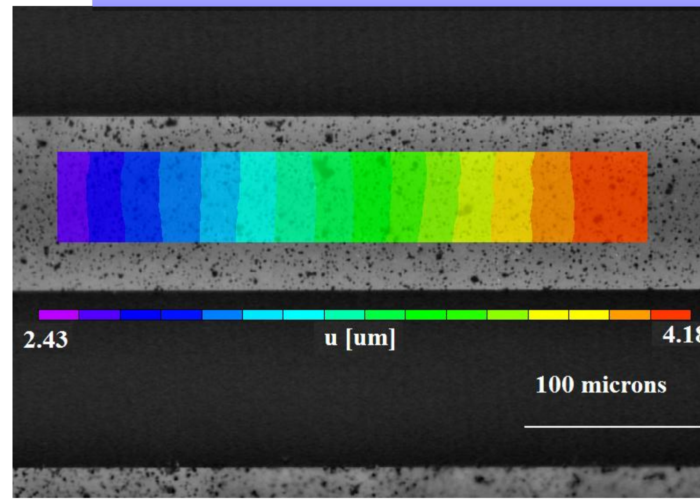

Transverse displacement field

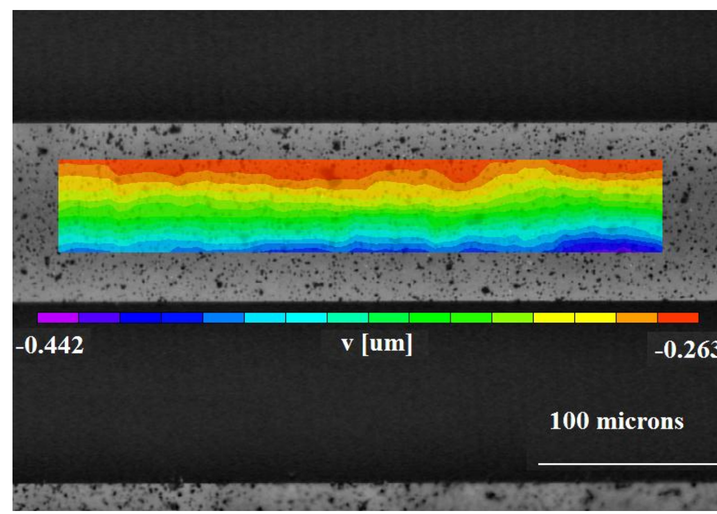

S. Yagnamurthy, I. Chasiotis, J. Lambros, R. Polcawich, J. Pulskamp, M. Dubey, “Mechanical and Ferroelectric Behavior of PZT Thin Films,” Journal of Microelectromechanical Systems 20, pp. 1250-1258, (2011).

Mechanical Behavior of SiO_2-Pt-PZT-Pt

Open circuit condition

Short circuit condition

PZT stack (open circuit)

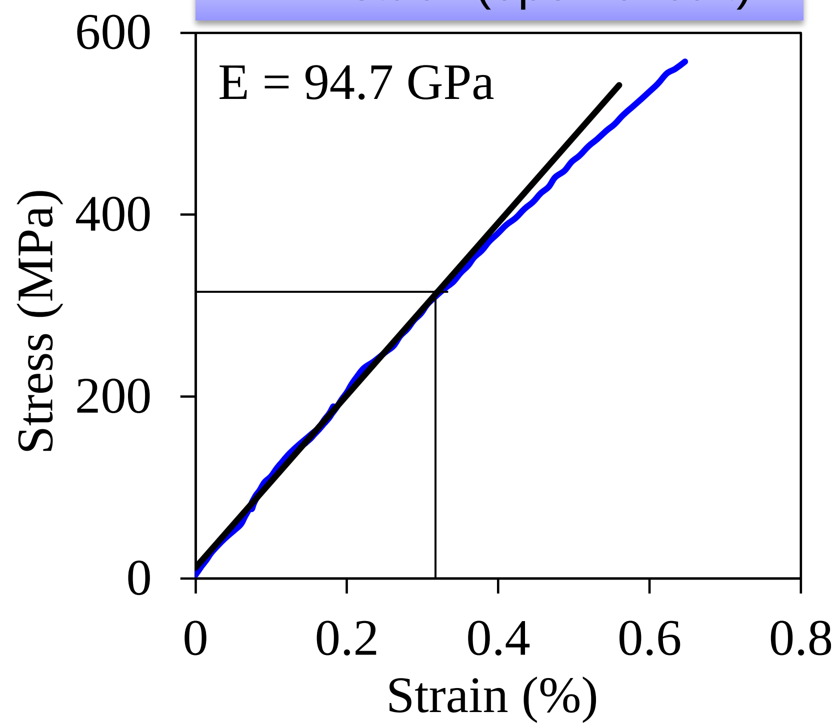

- Stress-strain curves were nonlinearly elastic with failure 0.6% strain
- Nonlinearity was attributed to domain switching mechanism in PZT at higher stresses

S. Yagnamurthy, I. Chasiotis, J. Lambros, R. Polcawich, J. Pulskamp, M. Dubey, "Mechanical and Ferroelectric Behavior of PZT Thin Films," Journal of Microelectromechanical Systems 20, pp. 1250-1258, (2011).

PZT Properties in Open and Short Circuit Conditions

PZT curves (extracted from laminas)

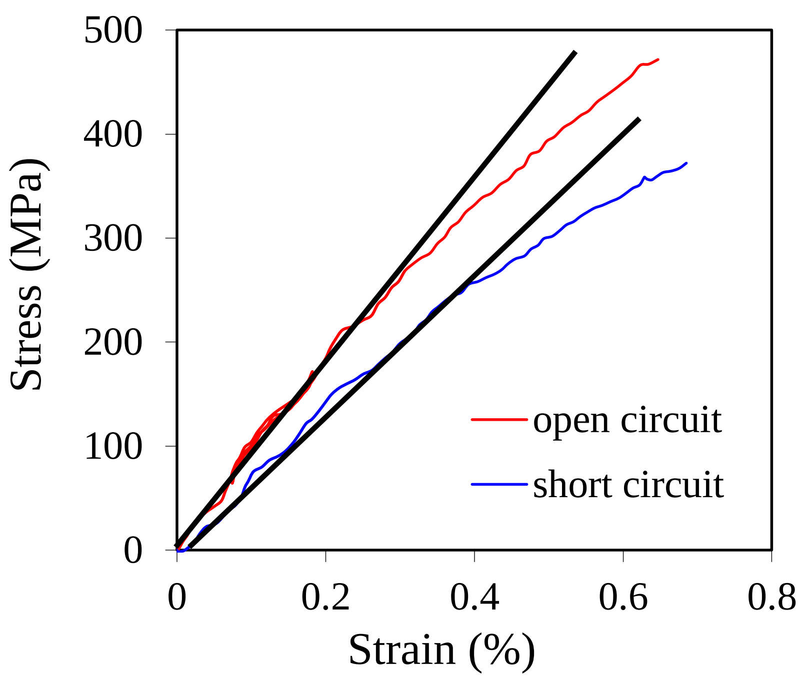

Material	Modulus (GPa)	$\sigma_{failure}$ (MPa)
SiO_2	72.3±2	1,170±200
SiO_2-Pt	87.9±1	780±70
Pt **	182±8	1,876±10
SiO_2-Pt-PZT	87.9±1	412±50
SiO_2-Pt-PZT-Pt	93.5±2.3	511±50
PZT (open circuit)	**84±3**	510±35
PZT (short circuit)	**60.5±5**	356±55

The modulus of PZT was extracted using simple laminate theory as 84±3 GPa and 60.5±5 GPa for open and short circuit conditions, respectively.

S. Yagnamurthy, I. Chasiotis, J. Lambros, R. Polcawich, J. Pulskamp, M. Dubey, "Mechanical and Ferroelectric Behavior of PZT Thin Films," Journal of Microelectromechanical Systems 20, pp. 1250-1258, (2011).

Ferroelectric Behavior at High Electric Fields (Low Voltage)

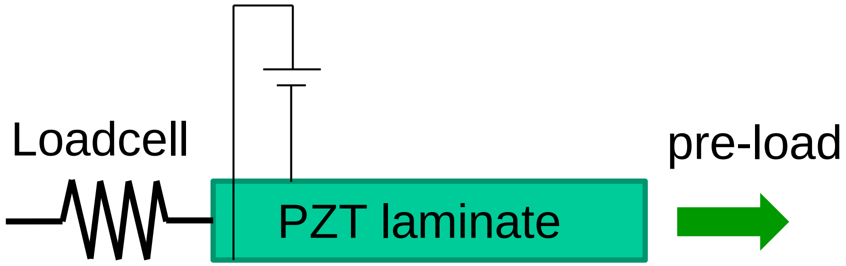

$\pm$10 V DC

- Electric field induced stress hysteresis loops were measured with applied pre-stress in the range of 0-600 MPa
- At high applied electric fields (> 2MV m^{-1}), the ferroelectric behavior of PZT is due to electrostriction and domain switching
- The electroactive coefficient, $e_{31,eff}$ was used to quantify the ferroelectric behavior of PZT as the ratio of stress to applied electric field:

$$P = e_{31,eff} \cdot \frac{V}{t_{PZT}} \cdot A_{PZT}$$

Effect of Applied Pre-Stress on Hysteresis Loops

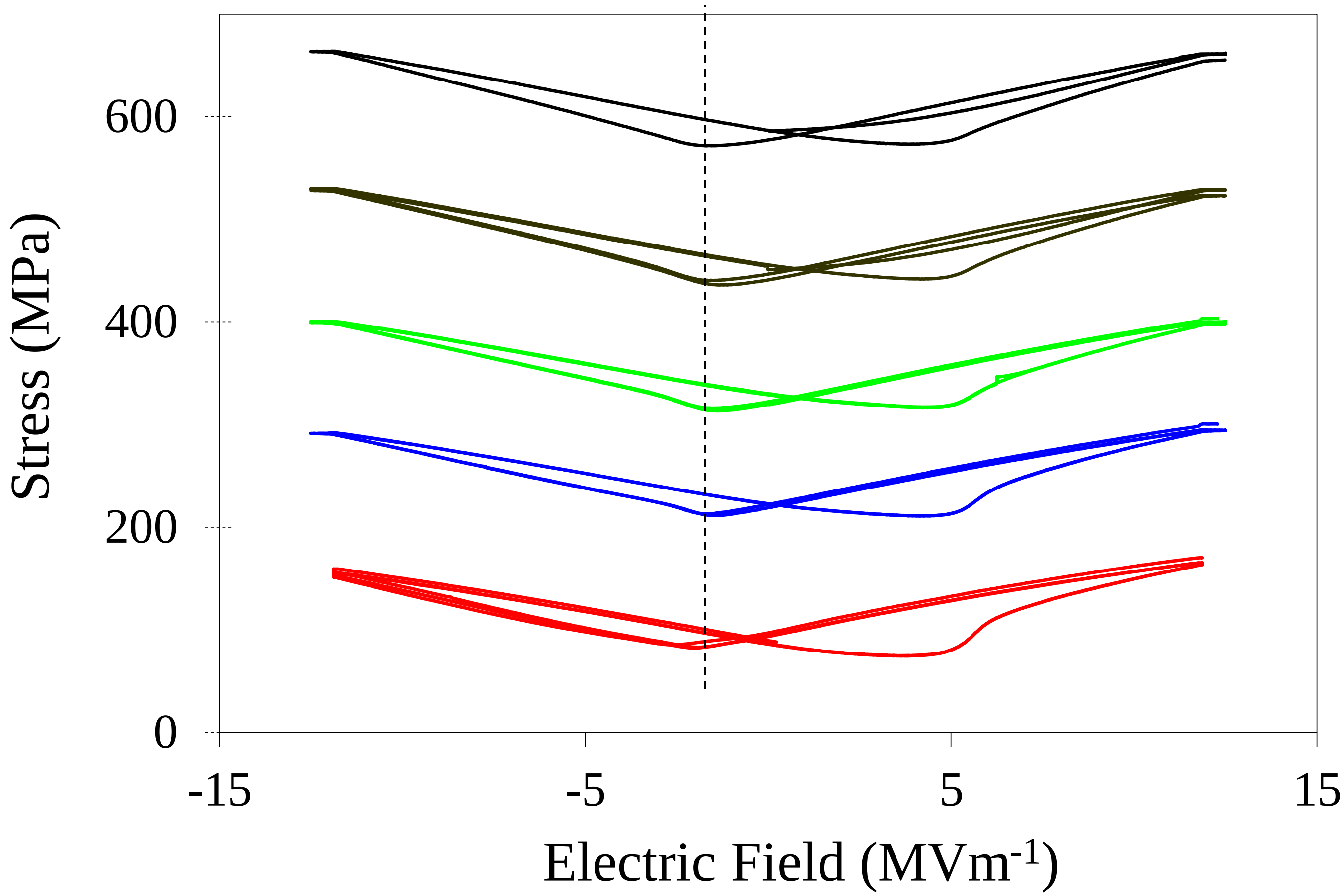

- Stress induced hysteresis loops became symmetric at high applied stresses
- The intersection of the hysteresis loops shifted to positive electric fields.

S. Yagnamurthy, I. Chasiotis, J. Lambros, R. Polcawich, J. Pulskamp, M. Dubey, "Mechanical and Ferroelectric Behavior of PZT Thin Films," Journal of Microelectromechanical Systems 20, pp. 1250-1258, (2011).

Dependence of Electroactive Coefficient on Pre-stress

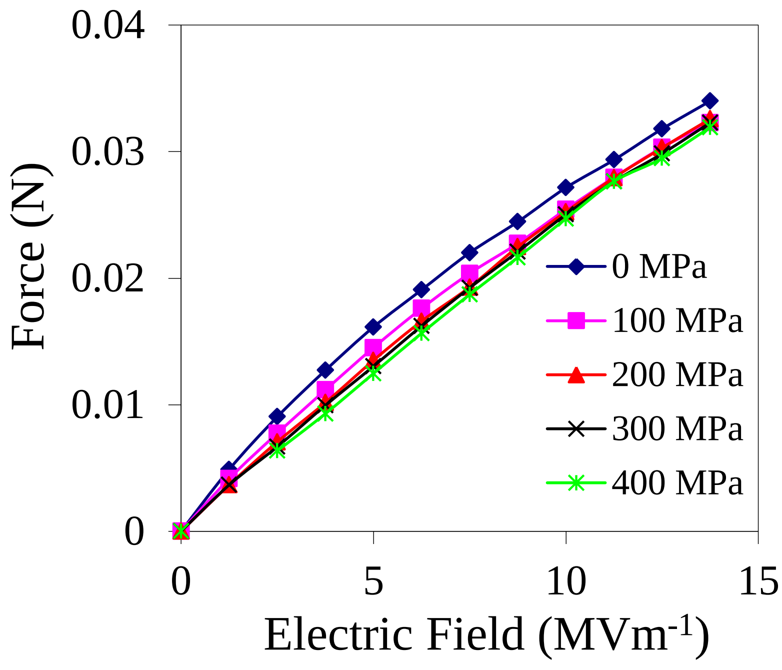

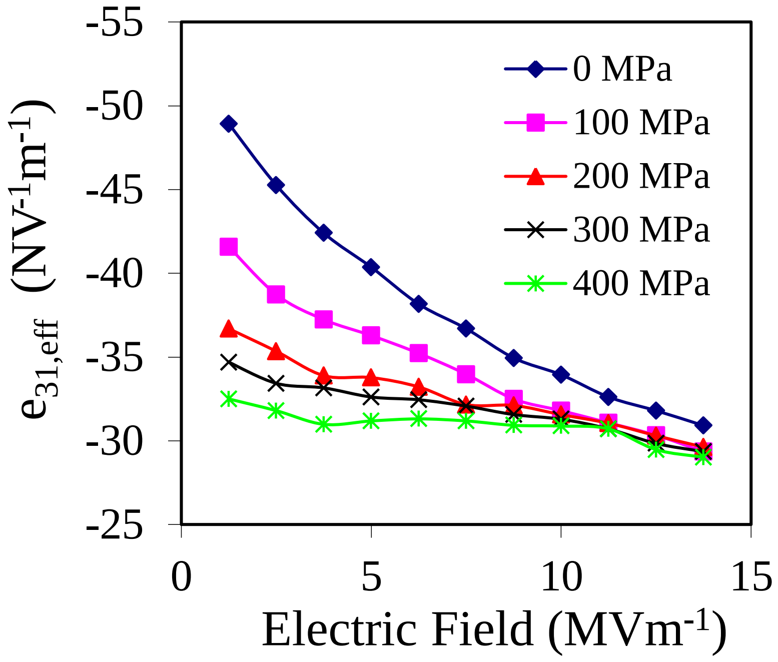

- With no pre-stress, $e_{31,eff}$ varied nonlinearly with applied electric field between -50 $NV^{-1}m^{-1}$ and -30 $NV^{-1}m^{-1}$ and was independent of the applied field at high pre-stress amplitudes.
- Pre-stress lowers domain switching activity in PZT and produces more linear actuation force with the applied electric field.

S. Yagnamurthy, I. Chasiotis, J. Lambros, R. Polcawich, J. Pulskamp, M. Dubey, "Mechanical and Ferroelectric Behavior of PZT Thin Films," Journal of Microelectromechanical Systems 20, pp. 1250-1258, (2011).

Conclusions

- Evaluated the effective mode I critical stress intensity factor for laminated and columnar grain polysilicon films as a function of dopant concentration to assess the role of grain heterogeneity and local toughness on crack initiation and arrest
- Quantified the effect of specimen size on fracture strength of polysilicon films via a Weibull analysis to identify the location of failure initiation
- Failure originates in patterning processes rather than deposition: Investigating the effect of removal of sidewall flaws on strength improvement
- Investigating the role of doping using bi-crystal experiments using chevron specimens
- Obtained the electroactive coefficients PZT thin films for MEMS and mechanical properties under open and short circuit conditions: They were the first data of their kind and have drawn interest by industry too.